

# CDM models with a steplike initial power spectrum

Mirt Gramann and Gert Hütsi

*Tartu Observatory, Tõravere 61602, Estonia*

21 August 2021

## ABSTRACT

We investigate the properties of clusters of galaxies in the  $\Lambda$ CDM models with a steplike initial power spectrum. We examine the mass function, the peculiar velocities and the power spectrum of clusters in models with different values of the density parameter  $\Omega_0$ , the normalized Hubble constant  $h$  and the spectral parameter  $p$ , which describes the shape of the initial power spectrum. The results are compared with observations. We also investigate the rms bulk velocity in the models, where the properties of clusters are consistent with the observed data. We find that the power spectrum of clusters is in good agreement with the observed power spectrum of the Abell-ACO clusters, if the spectral parameter  $p$  is in the range  $p = 0.6 - 0.8$ . The power spectrum and the rms peculiar velocity of clusters are consistent with observations only if  $\Omega_0 < 0.4$ . The  $\Omega_0 = 0.3$  models are consistent with the observed properties of clusters, if  $h = 0.50 - 0.63$ . For  $h = 0.65$ , we find that  $\Omega_0 = 0.20 - 0.27$ .

**Key words:** cosmology: theory – large-scale structure of Universe, cosmology: theory – dark matter, galaxies: clusters

## 1 INTRODUCTION

The theory of galaxy formation based on gravitational instability describes how primordially generated fluctuations grow into galaxies and clusters of galaxies due to self-gravity of matter. The initial field of density fluctuations  $\delta(\mathbf{x}, t)$  can be decomposed into its Fourier components  $\delta_{\mathbf{k}}(t)$  and expressed in terms of the power spectrum  $P(k) = \langle |\delta_{\mathbf{k}}|^2 \rangle$ .

As the study of the large-scale structure in the Universe has pushed to ever larger scales, several data samples have suggested the presence of a peak in the power spectrum at the wavenumber  $k \simeq 0.05h \text{ Mpc}^{-1}$  (or at the wavelength  $\lambda \simeq 120 - 130h^{-1} \text{ Mpc}$ ). Einasto et al. (1997) and Retzlaff et al. (1998) studied the spatial distribution of the Abell-ACO clusters and found that the power spectrum of the clusters has a well-defined peak at the wavenumber  $k = 0.052h \text{ Mpc}^{-1}$ . A similar peak in the one-dimensional power spectrum of a deep pencil-beam survey was detected by Broadhurst et al. (1990), and in the two-dimensional power spectrum of the Las Campanas redshift survey by Landy et al. (1996). The power spectrum of the spatial distribution of APM galaxies also has a feature on the same scale (Caztanaga and Baugh 1998). Independent evidence for the presence of a preferred scale in the Universe at about  $130h^{-1} \text{ Mpc}$  comes from an analysis of high-redshift galaxies. Broadhurst and Jaffe (1999) studied the distribution of the Lyman-break galaxies at redshift  $z \sim 3$  and found a  $5\sigma$  excess of pairs separated by  $\Delta z = 0.22 \pm 0.02$ , equivalent to  $130h^{-1} \text{ Mpc}$  for flat universe with the density parameter  $\Omega_0 = 0.4 \pm 0.1$ .

The power spectrum of density fluctuations depends on the physical processes in the early universe. The peak in the power spectrum of clusters at the wavenumber  $k \simeq 0.05h \text{ Mpc}^{-1}$  may be generated during the era of radiation domination or earlier. Standard cosmological models based on collisionless dark matter [e.g. cold dark matter (CDM)] and adiabatic fluctuations, when combined with power-law initial power spectra, predict smooth power spectra of density fluctuations at  $z \sim 10^3$ . The baryonic acoustic oscillations in adiabatic models may explain the observed power spectrum only if currently favored determinations of cosmological parameters are in substantial error (e.g., if the density parameter  $\Omega_0 < 0.2h$ ; Eisenstein et al. 1998).

One possible explanation for the observed power spectrum of clusters is an inflationary model with a scalar field whose potential  $V(\varphi)$  has a local steplike feature in the first derivative. This feature can be produced by a fast phase transition in a physical field different from the inflaton field. An exact analytical expression for the scalar (density) perturbations generated in this inflationary model was found by Starobinsky (1992). The initial power spectrum of density fluctuations in this model can be expressed as

$$P_{in}(k) \propto \frac{k S(k, p)}{p^2}, \quad (1)$$

where the function  $S(k, p)$  can be written as

$$S(k, p) = 1 - \frac{3(p-1)}{y} \left[ f_1(y) \sin 2y + \frac{2}{y} \cos 2y \right] +$$

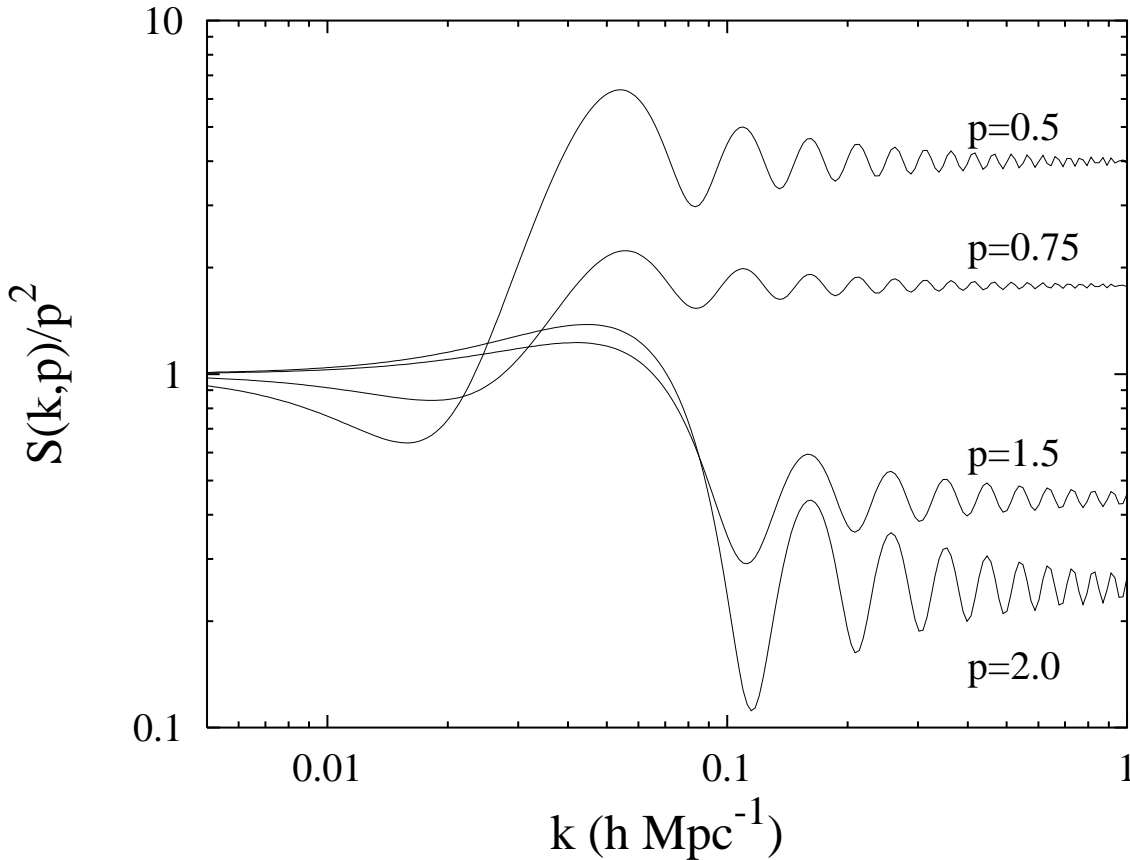


**Figure 1.** The function  $S(k,p)/p^2$  for different values of the parameter  $p$ . For the models with  $p < 1$  and  $p > 1$ , the step parameter was chosen to be  $k_0 = 0.016h \text{ Mpc}^{-1}$  and  $k_0 = 0.03h \text{ Mpc}^{-1}$ , respectively.

$$+ \frac{9(p-1)^2 f_2(y)}{2y^2} \left[ f_2(y) + f_1(y) \cos 2y - \frac{2}{y} \sin 2y \right]. \quad (2)$$

Here, the function  $y = k/k_0$ ,  $f_1(y) = 1 - y^{-2}$  and  $f_2(y) = 1 + y^{-2}$ . The initial power spectrum in this model depends on two parameters  $k_0$  and  $p$ . The parameter  $k_0$  determines the location of the step and the parameter  $p$  - the shape of the initial spectrum. For  $p = 1$ , we recover the scale-invariant Harrison-Zel'dovich spectrum ( $S(k,1) \equiv 1$ ). At present, the initial spectrum (1,2) is probably the only example of an initial power spectrum with the desired properties, for which a closed analytical form exists.

Fig. 1 shows the function  $S(k,p)/p^2$  for different values of the parameter  $p$ . For the models with  $p < 1$  and  $p > 1$ , the step parameter was chosen to be  $k_0 = 0.016h \text{ Mpc}^{-1}$  and  $k_0 = 0.03h \text{ Mpc}^{-1}$ , respectively. In this case, in the models with  $p < 1$ , the power spectrum has a well-defined maximum at the wavenumber  $k \simeq 0.05h \text{ Mpc}^{-1}$  and a second maximum at  $k \simeq 0.1h \text{ Mpc}^{-1}$ . In the models with  $p > 1$ , the picture is inverted. The power spectrum has a flat upper plateau at the wavenumbers  $k < 0.05h \text{ Mpc}^{-1}$ , a sharp decrease on smaller scales ( $k = 0.05 - 0.1h \text{ Mpc}^{-1}$ ) and a secondary maximum at  $k \simeq 0.15h \text{ Mpc}^{-1}$ .

Lesgourgues, Polarski & Starobinsky (1998, hereafter LPS) compared the CDM models with a steplike initial spectrum (1,2) with observational data. They studied the rms

mass fluctuation on an  $8h^{-1} \text{ Mpc}$  scale,  $\sigma_8$ ; the rms bulk velocity of galaxies and the cosmic microwave background (CMB) anisotropies on different angular scales. In this paper we continue this research and investigate the properties of galaxy clusters in these models. We examine the mass function, the peculiar velocities and the power spectrum of clusters for different values of the density parameter  $\Omega_0$ , the normalized Hubble constant  $h$  and the spectral parameter  $p$ . The results are compared with observations. We also investigate the rms bulk velocity and  $\sigma_8$  in the models, where the mass function, the peculiar velocities and the power spectrum of clusters are consistent with the observed data.

In their study LPS assumed that the parameter  $\sigma_8$  lies in the interval  $\sigma_8 = (0.57 \pm 0.06)\Omega_0^{-0.56}$ . This interval was derived by White, Efstathiou & Frenk (1993) by analysing the mass function of clusters. For  $\Omega_0 = 0.3$  this gives  $\sigma_8 = 1.0 - 1.25$ . In this paper we examine the observed values of the mass function of galaxy clusters in more detail and obtain lower values for the parameter  $\sigma_8$ . For  $\Omega_0 = 0.3$  we find that  $\sigma_8 = 0.8 - 1.05$ . Therefore, the allowed values for the parameter  $p$  in the  $(\Omega_0, h)$  plane that we obtain are different from those found by LPS.

We examine flat cosmological models with the density parameter  $\Omega_0 = 0.2 - 0.5$  and the normalized Hubble constant  $h = 0.5 - 0.8$ . These parameters are in agreement with

measurements of the density parameter (e.g. Bahcall et al. 1999) and with measurements of the Hubble constant using various distance indicators (e.g. Tammann 1998). To restore the spatial flatness in the low-density models, we assume a contribution from a cosmological constant:  $\Omega_\Lambda = 1 - \Omega_0$ . The Hubble constant is written as  $H_0 = 100h$  km s<sup>-1</sup>Mpc<sup>-1</sup>. The transfer function  $T(k)$  is computed with the fast Boltzmann code CMBFAST developed by Seljak & Zaldarriaga (1996). The models are normalized using the COBE normalization derived by Bunn & White (1997). We assume that the initial density fluctuation field in the Universe is a Gaussian field. In this case, the power spectrum provides a complete statistical description of the field.

This paper is organized as follows. In Section 2 we study the mass function of clusters of galaxies and compare the results with observations. In Section 3 we examine the peculiar velocities of galaxy clusters. In Section 4 we investigate the power spectrum of clusters. Discussion and summary are presented in Section 5.

## 2 THE MASS FUNCTION OF CLUSTERS OF GALAXIES

To study the mass function of clusters we use the Press-Schechter (1974, PS) approximation. The PS mass function has been compared with N-body simulations (Efstathiou et al. 1988; White, Efstathiou & Frenk 1993; Lacey & Cole 1994; Eke, Cole & Frenk 1996; Borgani et al. 1997a) and has been shown to provide an accurate description of the abundance of virialized cluster-size halos. In the PS approximation the number density of clusters with the mass between  $M$  and  $M + dM$  is given by

$$n(M)dM = -\sqrt{\frac{2}{\pi}} \frac{\rho_b}{M} \frac{\delta_t}{\sigma^2(M)} \frac{d\sigma(M)}{dM} \exp\left[-\frac{\delta_t^2}{2\sigma^2(M)}\right] dM. \quad (3)$$

Here  $\rho_b$  is the mean background density and  $\delta_t$  is the linear theory overdensity for a uniform spherical fluctuation which is now collapsing;  $\delta_t = 1.686$  for  $\Omega_0 = 1$ , with a weak dependence on  $\Omega_0$  for flat and open models (Eke et al. 1996; Kitayama & Suto 1996). In this paper we will use values of  $\delta_t$  found by Eke et al. (1996) for flat models. The function  $\sigma(M)$  is the rms linear density fluctuation at the mass scale  $M$ . We will use the top-hat window function to describe halos. For the top-hat window, the mass  $M$  is related to the window radius  $R$  as  $M = 4\pi\rho_b R^3/3$ . In this case, the number density of clusters of mass larger than  $M$  can be expressed as

$$n_{cl}(> M) = \int_M^\infty n(M')dM' = -\frac{3}{(2\pi)^{3/2}} \int_R^\infty \frac{\delta_t}{\sigma^2(r)} \frac{d\sigma(r)}{dr} \exp\left[-\frac{\delta_t^2}{2\sigma^2(r)}\right] \frac{dr}{r^3}. \quad (4)$$

Fig. 2 shows the cluster mass function in the flat models with  $\Omega_0 = 0.3$  and  $h = 0.65$ . The threshold density  $\delta_t = 1.675$ . We investigated the cluster masses within a  $1.5h^{-1}$  Mpc radius sphere around the cluster center. This

mass  $M_{1.5}$ , is related to the window radius  $R$  as

$$R = 8.43\Omega_0^{\frac{0.2\alpha}{3-\alpha}} \left[ \frac{M_{1.5}}{6.99 \times 10^{14}\Omega_0 h^{-1}M_\odot} \right]^{\frac{1}{3-\alpha}} (h^{-1}\text{Mpc}). \quad (5)$$

Here the parameter  $\alpha$  describes the cluster mass profile,  $M(r) \sim r^\alpha$ , at radii  $r \sim 1.5h^{-1}$  Mpc. Numerical simulations and observations of clusters indicate that the parameter  $\alpha \approx 0.6 - 0.7$  for most of clusters (Navarro, Frenk & White 1995; Carlberg, Yee & Ellingson 1997). In this paper we use a value  $\alpha = 0.65$ .

Fig. 2 shows also the mass function of clusters of galaxies derived by Bahcall and Cen (1993, BC) and by Girardi et al. (1998, G98). BC used both optical and X-ray observed properties of clusters to determine the mass function of clusters. The function was extended towards the faint end using small groups of galaxies. G98 determined the mass function of clusters by using virial mass estimates for 152 nearby Abell-ACO clusters including the ENACS data (Katgert et al. 1998). The mass function derived by G98 is somewhat larger than the mass function derived by BC, the difference being larger at larger masses (see Fig. 2).

Let us consider the amplitude of the mass function of galaxy clusters at  $M_{1.5} = 4 \cdot 10^{14}h^{-1}M_\odot$ . For this mass, the cluster abundances derived by BC and G98 are  $n(> M) = (2.0 \pm 1.1) \cdot 10^{-6}h^3 \text{ Mpc}^{-3}$  and  $n(> M) = (6.3 \pm 1.2) \cdot 10^{-6}h^3 \text{ Mpc}^{-3}$ , respectively. By analysing X-ray properties of clusters, White, Efstathiou & Frenk (1993) found that the number density of clusters with the mass  $M_{1.5} \approx 4.2 \cdot 10^{14}h^{-1}M_\odot$  is  $n(> M) = 4 \cdot 10^{-6}h^3 \text{ Mpc}^{-3}$ .

We derived the limits for the parameter  $p$ , assuming that the mass function of galaxy clusters at  $M_{1.5} = 4 \cdot 10^{14}h^{-1}M_\odot$  is in the range  $(2 - 6.5) \cdot 10^{-6}h^3 \text{ Mpc}^{-3}$ . Fig. 3a shows the results for the models with  $h = 0.65$  for different  $\Omega_0$  and Fig. 3b for the models with  $\Omega_0 = 0.3$  for different  $h$ . For the model with  $\Omega_0 = 0.3$  and  $h = 0.65$ , we find that  $p = 0.79 - 1.0$ . Fig. 2 demonstrates the mass function of clusters in this model for  $p = 0.79$  and  $p = 1.0$ .

LPS used high values of the parameter  $\sigma_8$  and found that one of the best-fit models is the model with parameters  $\Omega_0 = 0.3$ ,  $h = 0.7$ ,  $p = 0.8$ . We find that the number density of clusters in this model is substantially higher than observed; for the mass  $M_{1.5} = 4 \cdot 10^{14}h^{-1}M_\odot$ , the cluster abundance  $n(> M) = 9.8 \times 10^{-6}h^3 \text{ Mpc}^{-3}$ . For  $\Omega_0 = 0.3$  and  $h = 0.7$ , the mass function of clusters is consistent with the observed data, if  $p = 0.88 - 1.13$ .

## 3 PECULIAR VELOCITIES OF CLUSTERS OF GALAXIES

The observed rms peculiar velocity of galaxy clusters has been studied in several papers (e.g. Bahcall, Gramann & Cen 1994, Bahcall and Oh 1996, Borgani et al. 1997b, Watkins 1997). In this paper we use the results obtained by Watkins (1997). He developed a likelihood method for estimating the rms peculiar velocity of clusters from line-of-sight velocity measurements and their associated errors. This method was applied to two observed samples of cluster peculiar velocities: a sample known as the SCI sample (Giovannelli et al. 1997) and a subsample of the Mark III catalog (Willick et al. 1997). Watkins (1997) found that the rms one-dimensional

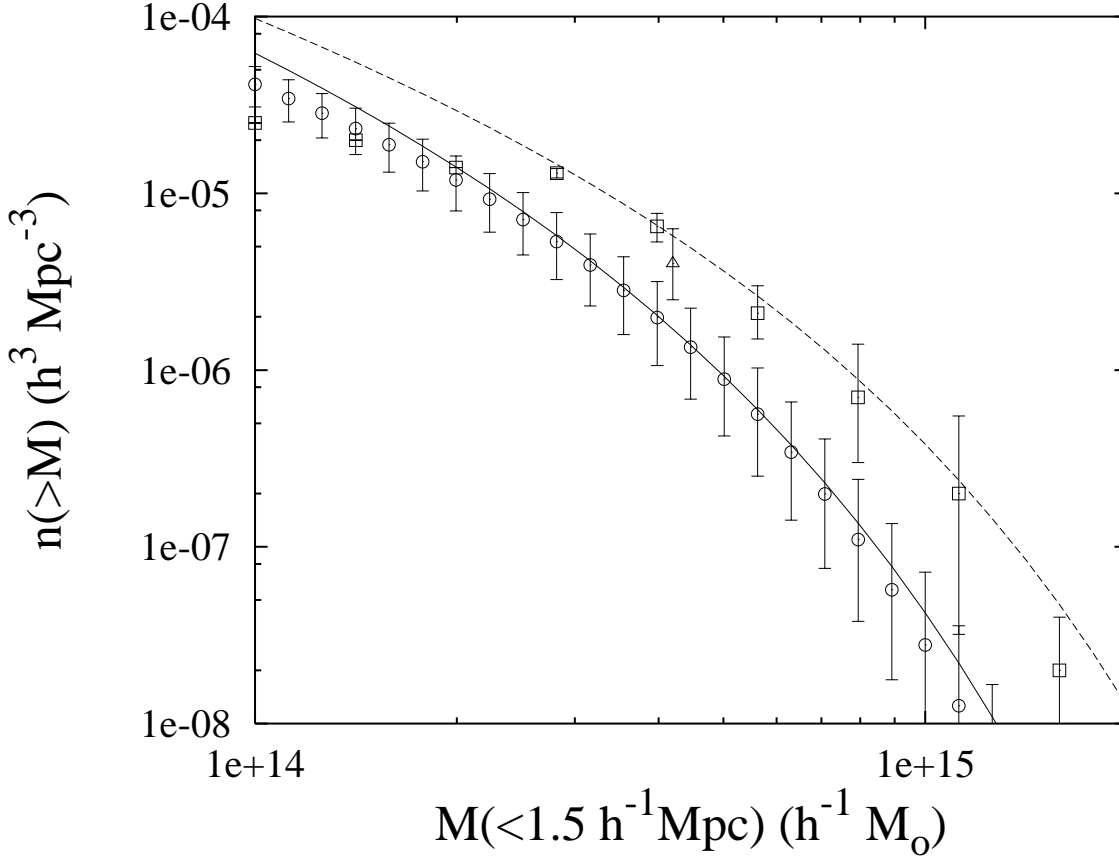


**Figure 2.** The cluster mass function in the models with  $\Omega_0 = 0.3$ ,  $h = 0.65$ ,  $p = 1.0$  (solid line) and  $p = 0.79$  (dashed line). Open circles and squares show the mass function of galaxy clusters derived by Bahcall and Cen (1993) and by Girardi et al. (1998), respectively. The open triangle is the result obtained by White, Efstathiou & Frenk (1993).

cluster peculiar velocity is  $265_{-75}^{+106}$  km s $^{-1}$ , which corresponds to the three-dimensional rms velocity  $459_{-130}^{+184}$  km s $^{-1}$ .

To investigate the peculiar velocities of clusters in our models, we use the linear theory predictions for peculiar velocities of peaks in the Gaussian field. The linear rms velocity fluctuation on a given scale  $R$  at the present epoch can be expressed as

$$\sigma_v(R) = H_0 f(\Omega_0) \sigma_{-1}(R), \quad (6)$$

where  $f(\Omega_0) \approx \Omega_0^{0.56}$  is the linear velocity growth factor in the flat models and  $\sigma_j$  is defined for any integer  $j$  by

$$\sigma_j^2 = \frac{1}{2\pi^2} \int P(k) W^2(kR) k^{2j+2} dk. \quad (7)$$

Bardeen et al. (1986) showed that the rms peculiar velocity at peaks of the smoothed density field differs systematically from  $\sigma_v(R)$ , and can be expressed as

$$\sigma_p(R) = \sigma_v(R) \sqrt{1 - \sigma_0^4 / \sigma_1^2 \sigma_{-1}^2}. \quad (8)$$

Suhhonenko & Gramann (1999) examined the linear theory predictions for the peculiar velocities of peaks and compared these to the peculiar velocities of clusters in N-body simulations. The N-body clusters were determined as peaks of the density field smoothed on the scale  $R \sim 1.5h^{-1}$

Mpc. The numerical results showed that the rms peculiar velocity of small clusters is similar to the linear theory expectations, while the rms peculiar velocity of rich clusters is higher than that predicted in the linear theory. The rms peculiar velocity of clusters with a mean cluster separation  $d_{cl} = 30h^{-1}$  Mpc was  $\sim 18$  per cent higher than that predicted by the linear theory. We assume that the observed cluster sample studied by Watkins (1997) corresponds to the model clusters with a separation  $d_{cl} \sim 30h^{-1}$  Mpc ( $n_{cl} \sim 3.7 \cdot 10^{-5} h^3$  Mpc $^{-3}$ ) and determine the rms peculiar velocity of the clusters,  $v_{cl}$ , as

$$v_{cl} = 1.18 \sigma_p(R), \quad (9)$$

where the radius  $R = 1.5h^{-1}$  Mpc.

Fig. 3 shows the limits for  $p$  in different models obtained on the basis of Watkins (1997) results. Fig. 3a shows the results in the  $h = 0.65$  models for different  $\Omega_0$  and Fig. 3b in the  $\Omega_0 = 0.3$  models for different  $h$ . In the region studied in Fig. 3b, the rms peculiar velocity is larger than 329 km s $^{-1}$ . For the model with  $\Omega_0 = 0.3$  and  $h = 0.65$ , we find that the initial parameter  $p > 0.87$ .

For high values of  $\Omega_0$  and  $h$ , peculiar velocities are larger than observed for any values of the parameter  $p$ . The velocities are sensitive to the amplitude of the large-scale

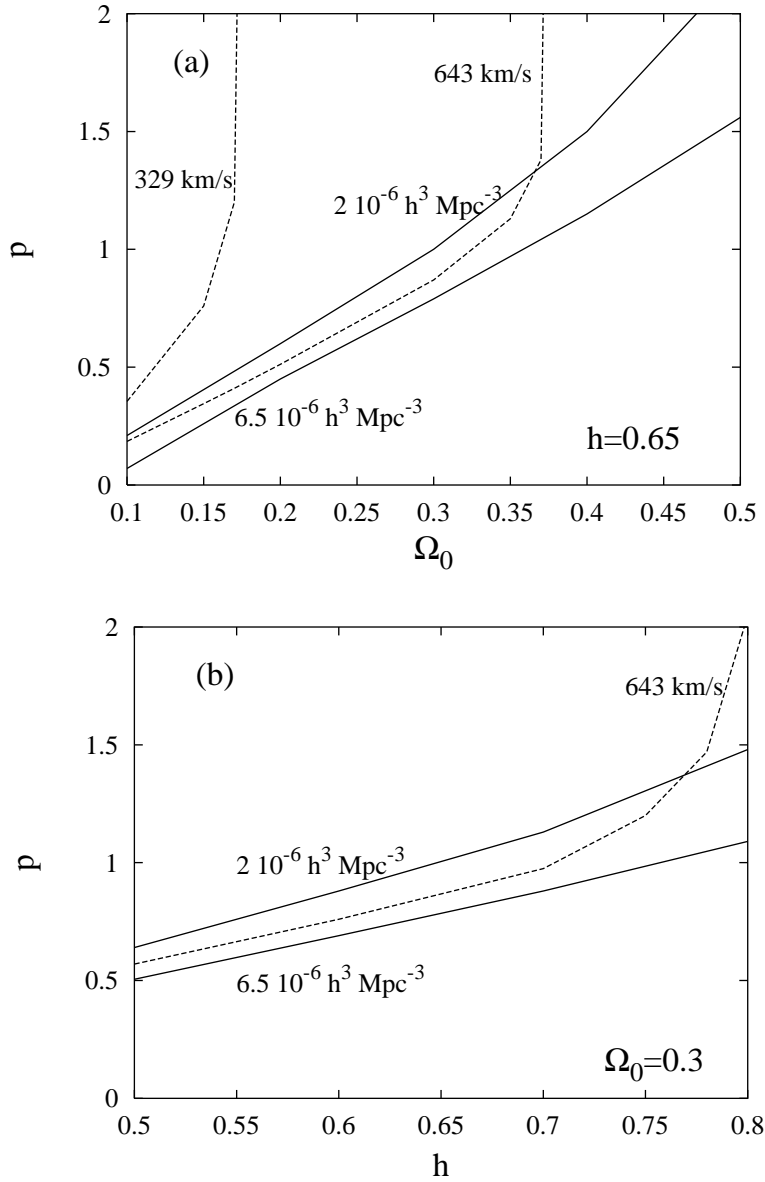


**Figure 3.** The limits for  $p$  in the  $\Lambda$ CDM models with a steplike initial power spectrum. Solid lines show the constraints obtained from the mass function of clusters and dashed lines show the constraints obtained by analysing the peculiar velocities of clusters. (a)  $h = 0.65$ . (b)  $\Omega_0 = 0.3$ . In the region studied peculiar velocities are larger than  $329 \text{ km s}^{-1}$ .

fluctuations at wavenumbers  $k < 0.1h \text{ Mpc}^{-1}$ . By increasing  $p$ , if  $p > 1$ , the power spectrum on these wavenumbers and, therefore, the velocities remain almost unchanged (see Fig. 1). Fig. 3a shows that in the  $h = 0.65$  models with  $\Omega_0 > 0.35$ , the peculiar velocities are not consistent with observations. For the  $\Omega_0 = 0.4$  model with  $h = 0.5$  and  $h = 0.6$ , we find that peculiar velocities are consistent with observations, if  $p > 0.86$  and  $p > 1.26$ , respectively.

If we compare the observational constraints obtained by studying the mass function and peculiar velocities of clusters of galaxies, we see from Fig. 3 that the mass function and the peculiar velocities of clusters are consistent with the

observed data only in a small interval of the parameter  $p$ . For the model with  $\Omega_0 = 0.3$  and  $h = 0.65$ , we find that  $p = 0.87 - 1.0$ . For the  $\Omega_0 = 0.3$  models with  $h = 0.5$  and  $h = 0.6$ , we find that  $p = 0.57 - 0.64$  and  $p = 0.76 - 0.88$ , respectively.

#### 4 THE POWER SPECTRUM OF CLUSTERS OF GALAXIES

Let us now consider the power spectrum of clusters in these models where both the mass function and the peculiar ve-

locities are consistent with observations. To investigate the power spectrum of clusters, we can also use the PS approach. The power spectrum of clusters for a given number density in the PS approximation can be expressed as (Gramann & Suhhonenko 1999, hereafter GS)

$$P_{cl}(k) = b_{cl}^2 P(k), \quad (9)$$

where the cluster bias parameter  $b_{cl}$  is

$$b_{cl} = 1 - \frac{3}{(2\pi)^{3/2} n_{cl}} \int_R^\infty \frac{1}{\sigma^2(r)} \frac{d\sigma(r)}{dr} (y^2 - 1) \exp(-y^2) \frac{dr}{r^3}. \quad (10)$$

Here, the function  $y = \delta_t/\sigma(r)$  and  $\sigma(r)$  is the rms linear density fluctuation at the radius  $r$ . The cluster bias parameter  $b_{cl}$  depends on the minimal mass  $M$  (or the window radius  $R$ ) of clusters and on the power spectrum of density fluctuations,  $P(k)$ , which determines the function  $\sigma(r)$ . For fixed  $P(k)$  and  $n_{cl}$ , the minimal mass  $M$  (or scale  $R$ ) can be determined by inverting equation (4).

Observations provide the distribution of clusters in redshift space, which is distorted due to peculiar velocities of clusters. On large scales, where linear theory applies, the power spectrum of matter density fluctuations in redshift space is given by (Kaiser 1987):

$$P^s(k) = \left[ 1 + \frac{2f(\Omega_0)}{3} + \frac{f^2(\Omega_0)}{5} \right] P(k). \quad (11)$$

Using the PS approximation (10), relation (11) takes the form

$$P_{cl}^s(k) = \left[ 1 + \frac{2f(\Omega_0)}{3b_{cl}} + \frac{f^2(\Omega_0)}{5b_{cl}^2} \right] b_{cl}^2 P(k). \quad (12)$$

Equation (12) determines the power spectrum of clusters for a given  $n_{cl}$  in redshift space.

GS examined the power spectrum of clusters in the PS theory and in N-body simulations. They determined the power spectrum of clusters for mean separations  $d_{cl} = 30 - 40h^{-1}$  Mpc. The numerical results showed that at wavenumbers  $k < 0.1h^{-1}$  Mpc, the power spectrum of clusters in the simulations is linearly enhanced with respect to the power spectrum of the matter distribution. However, the amplitude of the spectrum of clusters was somewhat lower than predicted by the approximation (12). It is possible that the linear approximation (12) overestimates the power spectrum of clusters due to dynamical effects that are not taken into account in this approximation. The power spectrum of clusters can be expressed as

$$P_{cl}^s(k) = F \left[ 1 + \frac{2f(\Omega_0)}{3b_{cl}} + \frac{f^2(\Omega_0)}{5b_{cl}^2} \right] b_{cl}^2 P(k), \quad (13)$$

where the factor  $F = 0.7 - 0.8$ . The factor  $F$  depends slightly on the model. GS examined the distribution of clusters in two cosmological models which start from the observed power spectra of the distribution of galaxies and clusters of galaxies. In the model (1), the initial linear power spectrum of density fluctuations was chosen in the form  $P(k) \propto k^{-2}$  at wavelengths  $\lambda < 120h^{-1}$  Mpc. In the model (2), GS assumed that the initial power spectrum contains a primordial feature at the wavelengths  $\lambda \sim 30 - 60h^{-1}$  Mpc. They found that  $F = 0.8$  and  $F = 0.7$  in the model (1) and model (2), respectively. In this paper we use a value  $F = 0.75$ .

Fig. 4 shows the redshift-space power spectrum of the

model clusters with a mean separation  $d_{cl} = 34h^{-1}$  Mpc. For comparison, we show the power spectrum of the Abell-ACO clusters determined by Einasto et al. (1999). This spectrum represents the weighted mean of the power spectra determined by Einasto et al. (1997) and Retzlaff et al. (1998). Einasto et al. (1997) determined the power spectrum of the Abell-ACO clusters from the correlation function of clusters, while Retzlaff et al. (1998) estimated the power spectrum directly (see Einasto et al. 1999 for details). The power spectrum of the distribution of the Abell-ACO clusters peaks at the wavenumber  $k = 0.052h$  Mpc $^{-1}$ . The mean intercluster separation of the Abell-ACO clusters is  $d_{cl} \sim 34h^{-1}$  Mpc ( $n_{cl} \sim 2.5 \cdot 10^{-5} h^3$  Mpc $^{-3}$ ) (Einasto et al. 1997, Retzlaff et al. 1998).

Fig. 4 shows the power spectrum of clusters predicted in the  $\Omega_0 = 0.3$  models with  $(h = 0.5, p = 0.6)$ ,  $(h = 0.6, p = 0.8)$ ,  $(h = 0.65, p = 0.95)$  and  $(h = 0.7, p = 1.05)$ . For these models, the mass function and the peculiar velocities are consistent with the observed data (see Fig. 3b). The models with  $p = 0.6$  and  $p = 0.8$  are in good agreement with the observed power spectrum, while the models with  $p = 0.95$  and  $p = 1.05$  are not consistent with the observed data. In the models with  $p > 0.95$ , we do not see a peak in the power spectrum at the wavenumber  $k \simeq 0.05h$  Mpc $^{-1}$ .

We used also the  $\chi^2$  test to calculate the probability that the models fit the observed power spectrum. The observed power spectrum represents the weighted mean of the power spectra determined by Einasto et al. (1997) and Retzlaff et al. (1998) and it is not clear how many points of the power spectrum are independent. As a first step we used all the data points in Fig. 4. The models with  $p = 0.6$  and  $p = 0.8$  are consistent with the observed power spectrum at a confidence level higher than 90%. For the models with  $p = 0.95$  and  $p = 1.05$ , the probability that the models fit the observed power spectrum is less than 30%.

We studied also the power spectrum of clusters in other models with different values of  $(\Omega_0, h)$  and found similar results. The power spectrum of clusters is in good agreement with the observed power spectrum of the Abell-ACO clusters, if the initial parameter  $p$  is in the range  $p = 0.6 - 0.8$ . In the models with  $h = 0.65$ , the allowed values for the parameter  $p$  are in this range, if  $\Omega_0 = 0.20 - 0.27$  (see Fig. 3a). Similarly, the  $\Omega_0 = 0.3$  models are consistent with the observed mass function, peculiar velocities and the power spectrum of clusters, if  $h = 0.50 - 0.63$  (Fig. 3b).

In the  $\Omega_0 = 0.4$  model with  $h = 0.5$ , the peculiar velocities are larger than observed, if  $p < 0.86$ . For higher values of  $\Omega_0$  and  $h$ , this limit for  $p$  increases. Therefore, for  $\Omega_0 \geq 0.4$  and  $h \geq 0.5$ , the observed power spectrum and peculiar velocities of clusters are not consistent with each other. Either the observed peculiar velocities are underestimated, or the observed peak in the power spectrum of clusters is overestimated. The peculiar velocities and the power spectrum of clusters are consistent with observations only if  $\Omega_0 < 0.4$ .

## 5 DISCUSSION AND SUMMARY

In this paper, we have examined the properties of clusters of galaxies in the  $\Lambda$ CDM models with a steplike initial power spectrum (1,2) that depends on two parameters  $k_0$  and  $p$ . The parameter  $k_0$  determines the location of the step and

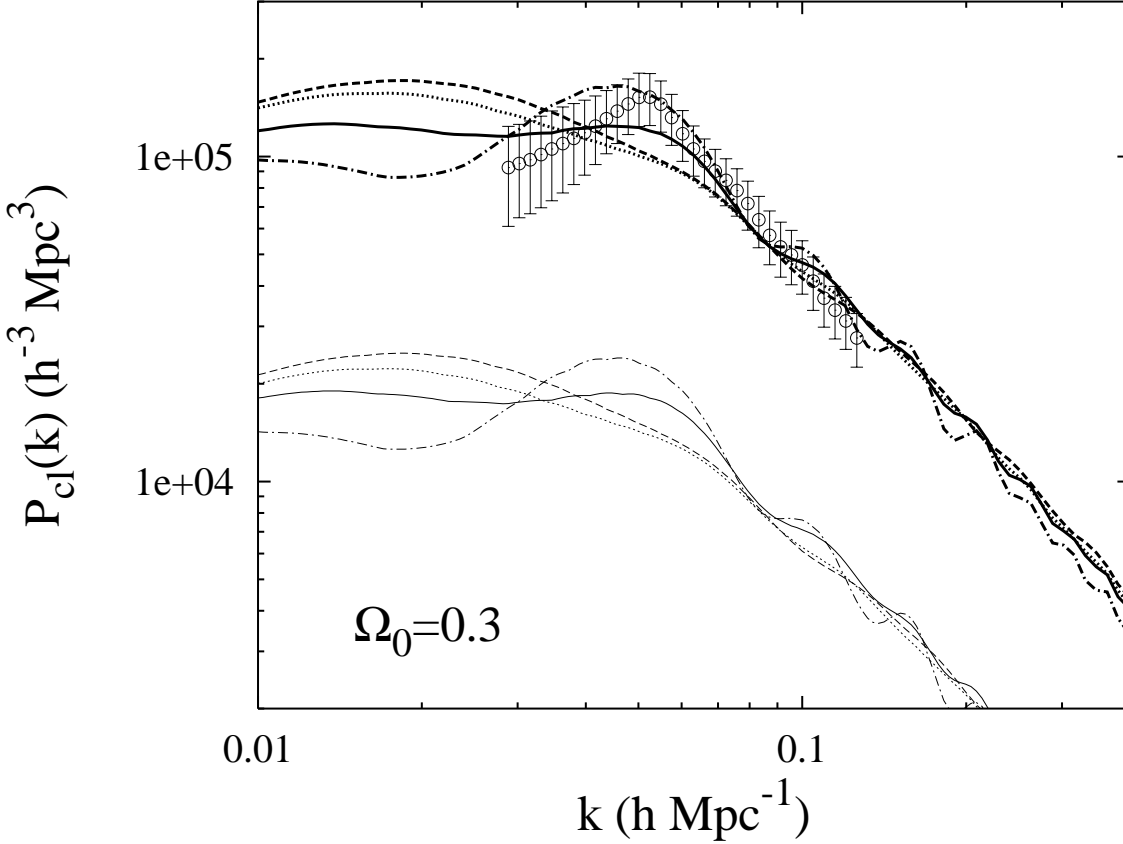


**Figure 4.** The power spectrum of the model clusters and the Abell-ACO clusters (open circles) with a separation  $d_{cl} = 34h^{-1}$  Mpc. The heavy lines show the power spectra of clusters determined by approximation (13) and the light lines the corresponding linear power spectra of matter fluctuations. We have shown the spectra for the  $\Omega_0 = 0.3$  models with  $h = 0.5$ ,  $p = 0.6$  (dot-dashed lines),  $h = 0.6$ ,  $p = 0.8$  (solid lines),  $h = 0.65$ ,  $p = 0.95$  (dotted lines) and  $h = 0.7$ ,  $p = 1.05$  (dashed lines).

the parameter  $p$  - the shape of the initial spectrum. For the models with  $p < 1$  and  $p > 1$ , the step parameter was chosen to be  $k_0 = 0.016h \text{ Mpc}^{-1}$  and  $k_0 = 0.03h \text{ Mpc}^{-1}$ , respectively. We investigated the mass function, peculiar velocities and the power spectrum of clusters in models with different values of  $\Omega_0$ ,  $h$  and  $p$ .

We found that the mass function and the peculiar velocities of clusters are consistent with the observed data only in a small interval of the parameter  $p$ . For the model with  $\Omega_0 = 0.3$  and  $h = 0.65$ , we find that  $p = 0.87 - 1.0$ . For the  $\Omega_0 = 0.3$  models with  $h = 0.5$  and  $h = 0.6$ , we find that  $p = 0.57 - 0.64$  and  $p = 0.76 - 0.88$ , respectively.

The power spectrum of clusters in the  $\Lambda$ CDM models with a steplike initial power spectrum is in good agreement with the observed power spectrum of the Abell-ACO clusters, if the initial parameter  $p$  is in the range  $p = 0.6 - 0.8$ . In the models with  $h = 0.65$ , the allowed values for the parameter  $p$  are in this range if  $\Omega_0 = 0.20 - 0.27$ . The  $\Omega_0 = 0.3$  models are consistent with the observed mass function, peculiar velocities and the power spectrum of clusters, if  $h = 0.50 - 0.63$ . The peculiar velocities and the power spectrum of clusters are consistent with observations only if  $\Omega_0 < 0.4$ .

We also studied the rms bulk velocity in the models,

where the mass function, the peculiar velocities and the power spectrum of clusters are consistent with observations. We chose three models in the allowed parameter space and studied these models in more detail. Table 1 lists the parameters of the models studied. We have determined the number density of clusters with mass  $M_{1.5} = 4 \cdot 10^{14} h^{-1} M_\odot$ ,  $n_{cl}$ ; the rms mass fluctuation on an  $8h^{-1}$  Mpc scale,  $\sigma_8$ ; the rms peculiar velocity of clusters,  $v_{cl}$ , and the rms bulk velocity for a radius  $r = 50h^{-1}$  Mpc,  $V_{50}$ . The rms bulk velocity was determined by using eq. (6). The observed bulk velocities are determined in a sphere centered on the Local Group and represent a single measurement of the bulk flow on large scales. The observed bulk velocity derived from the Mark III catalog of peculiar velocities for  $r = 50h^{-1}$  Mpc is  $375 \pm 135 \text{ km s}^{-1}$  (Kolatt & Dekel 1997). In the models studied, the rms bulk velocity is  $\sim 270 - 285 \text{ km s}^{-1}$ , which is consistent with the observed data.

Therefore, in many aspects the  $\Lambda$ CDM models with a steplike initial spectrum fit the observed data. Further work is needed to study the properties of galaxies and clusters of galaxies in these models in more detail.

**Table 1.** Results of the tests for the different models.

$\Omega_0$	$h$	$p$	$n_{cl}$ ( $10^{-6}h^3 \text{ Mpc}^{-3}$ )	$\sigma_8$	$v_{cl}$ ( $\text{km s}^{-1}$ )	$V_{50}$ ( $\text{km s}^{-1}$ )
0.20	0.75	0.70	2.9	1.05	610	270
0.25	0.65	0.75	2.8	0.95	610	270
0.30	0.60	0.80	3.3	0.90	635	285

**ACKNOWLEDGEMENTS**

We thank A. Starobinsky, J. Einasto and E. Saar for useful discussions. This work has been supported by the ESF grant 3601.

Willick, J.A., Courteau S., Faber, S. M., Burstein, D., Dekel, A., Strauss, M. A., 1997, *ApJS*, 109, 333

**REFERENCES**

- Bahcall, N.A., Cen, R. 1993, *ApJ*, 407, L49 (BC)  
Bahcall, N.A., Gramann, M., Cen, R. 1994, *ApJ*, 436, 23  
Bahcall, N.A., Oh, S.P. 1996, *ApJ*, 462, L49  
Bahcall, N.A., Ostriker, J.P., Perlmutter, S., Steinhardt, P.J. 1999, *Science*, 1481  
Bardeen, J.M., Bond, J.R., Kaiser, N., Szalay, A.S. 1986, *ApJ*, 304, 15  
Borgani, S. et al. 1997a, *NewA*, 1, 321  
Borgani, S., Da Costa L.N., Freudling, W., Giovanelli, R., Haynes, M.P., Salzer, J., Wegner, G., 1997b, *ApJ*, 482, L121  
Broadhurst, T.J., Ellis, R.S., Koo, D.S., Szalay, A.S. 1990, *Nature*, 343, 726  
Broadhurst, T.J., Jaffe, A. H., 1999, *ApJ*, submitted (astro-ph:9904348)  
Bunn, E.F., White, M. 1997, *ApJ*, 480, 6  
Carlberg, R.G., Yee, H.K.C., Ellingson, E. 1997, *ApJ*, 479, L19  
Caztanaga, E., Baugh, C.M. 1998, *MNRAS*, 294, 229  
Efstathiou, G., Frenk, C.S., White, S.D.M., Davis, M. 1988, *MNRAS*, 235, 715  
Einasto, J., et al. 1997, *Nature*, 385, 139  
Einasto, J., et al. 1999, *ApJ*, 519, 441  
Eisenstein, D.J., Hu, W., Silk, J., Szalay, A.S. 1998, *ApJ*, 494, L1  
Eke, V. R., Cole, S., Frenk, C. S. 1996, *MNRAS*, 282, 263  
Giovanelli, R. et al. 1997, *AJ*, 113, 22  
Girardi, M., Borgani, S., Giuricin, G., Mardirossian, F., Mezetti, M. 1998, *ApJ*, 506, 45 (G98)  
Gramann, M., Suhhonenko, I. 1999, *ApJ*, 519, 433  
Kaiser, N., 1987, *MNRAS*, 227, 1  
Katgert, P., Mazure, A., den Hartog, R., Adami, C., Biviano, A., Perea, J., 1998, *A & AS*, 129, 399  
Kitayama, T., Suto, Y. 1996, *ApJ*, 469, 480  
Kolatt, T., Dekel, A., 1997, *ApJ*, 479, 592  
Lacey, C., Cole, S. 1994, *MNRAS*, 271, 676  
Landy, S.D., Shectman, S.A., Lin, H., Kirshner, R.P., Oemler, A., Tucker, D., Schechter, P.L. 1996, *ApJ*, 456, L1  
Lesgourgues, J., Polarski, D., Starobinsky, A.A., 1998, *MNRAS*, 297, 769 (LPS)  
Navarro, J.F., Frenk, C.S., White, S.D.M. 1996, *ApJ*, 462, 563  
Press, W.H., Schechter, P. 1974, *ApJ*, 187, 425  
Retzlaff, J., Borgani, S., Gottlöber, S., Klypin, A., Müller, V. 1998, *New A*, 3, 631  
Seljak, U., Zaldarriaga, M., 1996, *ApJ*, 469, 7  
Starobinsky, A.A., 1992, *JETP Lett.*, 55, 477  
Suhhonenko, I., Gramann, M., 1999, *MNRAS*, 303, 77  
Tammann, G., 1998, in *General Relativity*, 8th Marcel Crossmann Symposium, ed. T. Piran, (Singapore:World Scientific)  
Watkins, R. 1997, *MNRAS*, 292, L59  
White, S. D. M., Efstathiou, G., & Frenk, C. S. 1993, *MNRAS*, 262, 1023